Dynamics of out-of-equilibrium electron and hole pockets in the type-II Weyl semimetal candidate WTe_{2}

M. Caputo, L. Khalil, E. Papalazarou, N. Nilforoushan, L. Perfetti, A. Taleb-Ibrahimi, Q. D. Gibson, R. J. Cava, and M. Marsi

Dynamics of out-of-equilibrium electron and hole pockets in the type-II Weyl semimetal candidate WTe$_2$

M. Caputo,[1, *] L. Khalil,[1, 2] E. Papalazarou,[1] N. Nilforoushan,[1] L. Perfetti,[3] A. Taleb-Ibrahimi,[4] Q. D. Gibson,[5] R. J. Cava,[5] and M. Marsi[1]

[1]*Laboratoire de Physique des Solides, CNRS, Université Paris-Sud, Université Paris-Saclay, 91405 Orsay Cedex, France*
[2]*Synchrotron SOLEIL, Saint Aubin BP 48, Gif-sur-Yvette F-91192, France*
[3]*Laboratoire des Solides Irradiés, Ecole Polytechnique, CNRS, CEA, Université Paris-Saclay, 91128 Palaiseau Cedex, France*
[4]*UR1-CNRS/Synchrotron SOLEIL, Saint Aubin BP 48, Gif-sur-Yvette F-91192, France*
[5]*Department of Chemistry, Princeton University, Princeton, New Jersey 08544, USA*
(Dated: February 21, 2018)

We present a time- and angular-resolved photoemission (TR-ARPES) study of the transition-metal dichalcogenide WTe$_2$, a candidate type II Weyl semimetal exhibiting extremely large magnetoresistence. Using femtosecond light pulses, we characterize the unoccupied states of the electron pockets above the Fermi level. Following the ultrafast carrier relaxation in distinct parts of the Brillouin zone, we report remarkably similar decay dynamics for electrons and holes. Our results confirm that charge compensation between electron and hole pockets – a key effect to explain the non saturating magnetoresistance of this material – is a distinctive feature of WTe$_2$ even in an out-of-equilibrium regime.

I. INTRODUCTION

Weyl semimetals establish a new class of quantum materials exhibiting topological protection[1–4]. A point-touching in reciprocal space between valence and conduction band creates Weyl nodes associated to a topologically protected charge (Fig. 1(a)). Their projection in the Fermi surface is point-like and the projection of nodes of opposite charge are connected with open surface states (Fermi Arcs)[5]. Recently, a new class of Weyl semimetals was proposed, namely the type-II Weyl semimetals[6], with Weyl points emerging from the linear crossing of electron and hole pockets. The Weyl fermion, in this case, is characterized by a Weyl cone that is tilted over one side (Fig. 1b). Violation of the Lorentz invariance in type-II Weyl semimetals is meant to lead to novel physical properties making these systems interesting to study[6].

Type-II Weyl fermions have been predicted to be found in some transition-metal dichalcogenides. WTe$_2$ and MoTe$_2$ are among the first type-II Weyl semimetal candidates under investigation[6–8]. High resolution ARPES measurements have successfully revealed surface states connecting hole and electron pockets in WTe$_2$[9–14] and Mo$_x$W$_{1-x}$Te$_2$[15–18] along with their complete spin polarization[19]. Despite intense efforts the topological nature of the surface states in these materials is still object of debate. TR-APRES experiments carried out on the unoccupied band structure of Mo-doped WTe$_2$ has unraveled arc-like surface states between the electron and hole pocket that could contain the topological states and, hence the Weyl points[20]. Despite the excellent agreement between the calculated band structure and the experiment, no direct spectroscopic signature has been actually observed. On the other hand, ultra-high resolution laser ARPES on thermally broadened WTe$_2$ showed a reach of surface states Fermi surface without, however, really conclusive results on its Weyl nature[10,21]. The Weyl points in this material reside above the Fermi level, thus making it difficult to be observed spectroscopically.
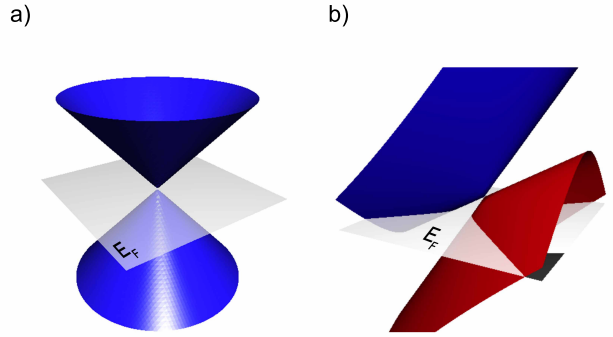
FIG. 1. (Color online) (a) Schematic illustration of the type-I Weyl semimetal with point-like Fermi surface (the case of monopnictide family), and (b) of type-II Weyl semimetal with tilted cone forming electron and hole pockets (the transition-metal dichalcogenide family).

The peculiar topology observed in various Dirac and Weyl materials has been proposed to be somehow related to their exceptional magnetotransport properties, like for instance the one found in Cd$_3$As$_2$[22] and in NbP[23]. WTe$_2$ has an extremely large, nonsaturating magnetoresistance at low temperatures and high magnetic fields[24]. The high magnitude of its magnetoresistance has been attributed to an almost perfect compensation between electrons and

holes and to the balanced arrangement of electron and hole pockets in the structure of the Fermi surface[9]. To date, a possible relation between these phenemona and the topological nature of its surface states has not been yet established.

In this paper, we report a time-resolved ARPES (TR-ARPES) study of WTe_2 single crystals. This technique makes it possible to explore the structure of empty electronic states, and to observe the carrier relaxation dynamics after the system has been driven out-of-equilibrium by femtosecond optical pulses. While our results cannot provide any conclusive evidence of Weyl nodes above the Fermi level, the relaxation dynamics of photoexcited states show a perfect balance between electrons and holes in the pockets at the proximity of the Fermi level.

II. METHODS

High quality WTe_2 single crystals were synthesized by the flux method as described elsewhere[24]. The pump-probe photoemission experiments have been performed at the FemtoARPES setup based on a commercial Ti:Sapphire laser delivering 35 fs pulses at 1.57 eV at a repetition rate of 250 kHz. Part of the output laser power was used to generate probe 6.28 eV photons through cascade frequency mixing in BBO crystals[25]. The energy and time resolution were estimated to be of $\approx$50 meV and 150 fs, respectively. The used pump fluence was 0.6 ± 0.02 mJ/cm^2 and the photoemission spectra were referred to the Fermi level (E_F) of the system at thermodynamic equilibrium. All samples were cleaved *in situ* at room temperature and base pressure of 1×10^{-10} mbar before being cooled down to 130 K.

III. RESULTS AND DISCUSSION

Figure 2(a) shows the Fermi surface as acquired with our system. With the help of the scheme in figure 2(b) the electron and hole pockets in the ΓX direction already reported by previous studies are easily recognizable.

Figures 2(c)-2(e) show cuts of constant momentum from pump-probe ARPES spectra probed with *s*-polarized UV light pulses at 350 fs after the arrival of the pump pulse, *i.e.* $\Delta t = 350$ fs. Cuts of the band structure along the high symmetry direction ΓX (see Fig. 2(c)) and at $k_y=0.05$ Å^{-1} (Fig. 2(d)) show clearly a broad electron-like band surrounded by a second band that creates the electron pocket below the Fermi level. Their dispersion moving away from the high symmetry direction, and the dispersion in the perpendicular direction reveal their paraboloid-like shape. At energies around 0.1-0.2 eV, the two bands expand over, pivoting on two distinct points located at [$k_x=0.23$ Å^{-1}, $k_y=\pm0.013$ Å^{-1}]: this is clearly shown in the video provided in supporting information[26], where a sequence of isoenergetic cuts at increasing E-E_F
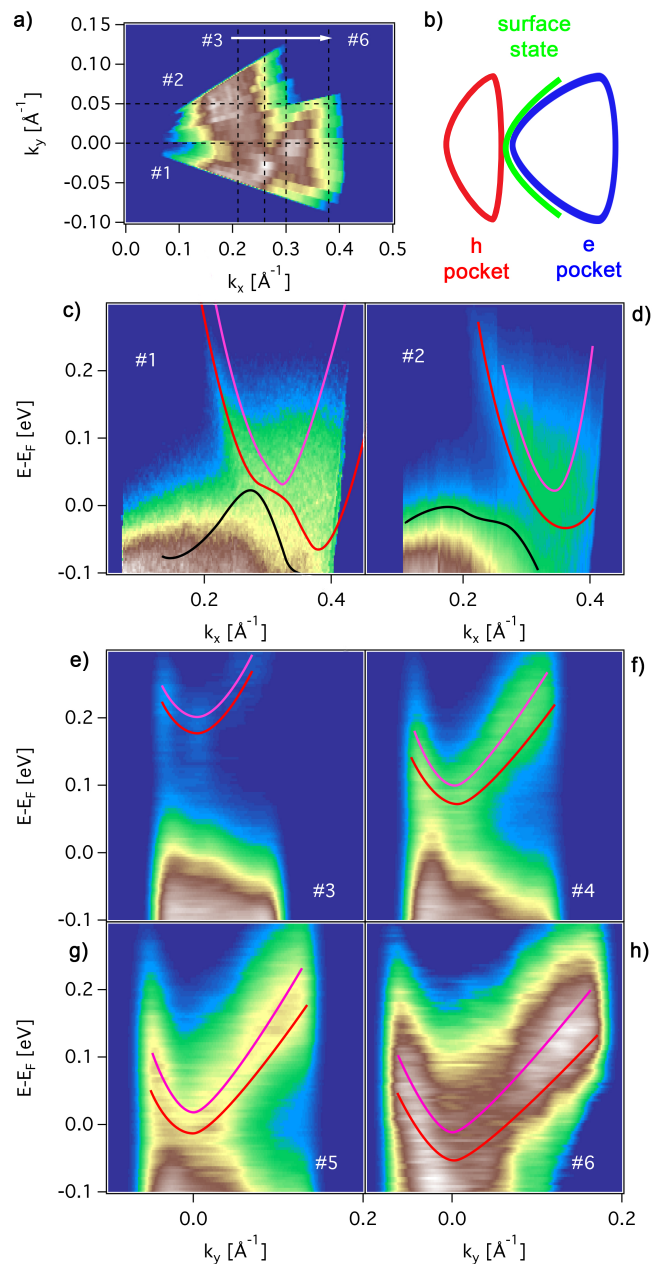
FIG. 2. (Color online) (a) Fermi surface of the WTe_2 along with its schematic illustration (b). Cuts along the high symmetry direction ΓX (c) and parallel to it (d), and cuts parallel to the high symmetry direction ΓY (e)-(h) (lines #1–#6 in (b)).

is shown. One might ask of whether we have a signature of Weyl points. From what we can tell, the overall band dispersion observed along these points and the fact that the band crossing happens well above the calculated position of the Weyl point suggests that this could not be a spectroscopic evidence of a Weyl semimetal. At this point, our experimental resolution does not permit us to make conclusive remarks on the topological nature of the observed surface states. Nevertheless, the analysis of the
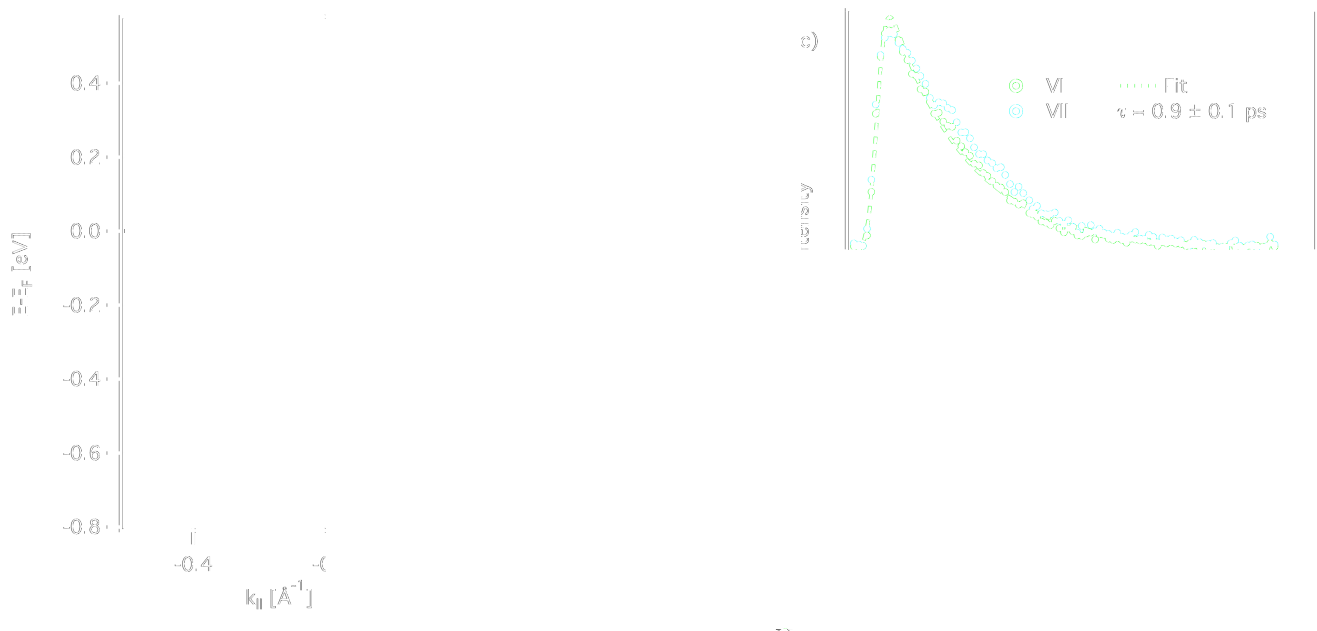
FIG. 3. (Color online) Cut of the band structure along the ΓX direction (panel a) together with the image difference ($\Delta t = 250$ fs - $\Delta t < 0$). Lines are guides to the eye showing the integration regions for the bands I-VII, whose normalized temporal evolution of carrier populations is reported in panels c and d. Panel e compared the decay dynamic of the region in the square containing presumably one of the Weyl points (WP), with a control region (C). Panel g compares the electrons and holes dynamic in the electrons and hole pockets T1 and T2 as defined in panel f.

system in the time domain provides interesting complementary information, in particular on the relaxation of photoexcited carriers.

Figure 3 shows the decay dynamics of photoexcited bands in WTe$_2$ acquired with p-polarized pulses along ΓX. Bands are labelled following the image shown in Fig. 3(b), *i.e.* the difference ARPES image acquired at $\Delta t = 250$ fs and an image at equilibrium, right before photoexcitation. Blue areas correspond to an electronic population depleted upon photoexcitation, while red areas correspond to an excess of electronic population. Our results are in fairly good agreement with previously reported calculations and measured band structures[9,11,27].

In order to follow the decay dynamics, seven regions are delineated as follows: five (I-V) below the Fermi level in correspondence of the occupied bands, and two above the Fermi level in correspondence of the two electron pockets (VI-VII). These regions have been chosen to follow the decay in a band-resolved manner: this can give

us insight in interband scattering process, and help in detecting singularities as Weyl points are[28–30]. Using the integration areas indicated in Figure S1[26], we can track the decay evolution of the carriers population of each band versus the pump-probe delay as shown in figures 3(c) and 3(d). At first glance, we can notice that both electron and hole populations decay exponentially, having similar decay times. Single exponential fits to bands VI and III give decay times of 0.9±0.1 ps and 1.2±0.3 ps, respectively (Fig. 3(b)). These values are in perfect agreement with previous time-resolved reflectivity experiments performed by Dai *et al.* on WTe$_2$[31].

Next, we compare the temporal evolution of the excess electronic population in two isoenergy regions around ∼30 meV above E_F marked as WP and C in Fig. 3(d). While both regions belong to the same electron pocket, WP region should contain the Weyl point according to previous reports[6], while C does not contain any singular point. Comparing the two areas will give us indication on

the effective presence of Weyl points in the region WP. From our measurements, one can notice a rapid intensity increase at WP shortly after photoexcitation reaching its maximum at $\Delta t \sim 350$ fs. We suggest that this behaviour is induced from impact ionization. Impact ionization in metals and semimetals is known to be the dominant scattering process for carrier relaxation leading to a multiplication of excess electrons at the vicinity of the Fermi level[32]. The process is k and band selective as it acts to minimize the total energy for any given charge carrier. In presence of a Dirac singularity, the extremely small density of states available for the carriers to cool down establishes a precursor of a population inversion, also known as "bottleneck effect", accumulating electrons and slowing down the charge recombination[29,33,34]. Nevertheless, the similar decay rates observed in WP and C does not give us any indication regarding the presence of a singularity (Weyl point) in the region WP.

Finally, we turn our attention to the comparison of the temporal evolution of the excess carrier densities in the vicinity of the Fermi level. This region is dominated by the presence of electron and hole pockets, and since these are the crucial players in the mechanism of non-saturating magnetoresistance, they are features of particular relevance. Figure 3(g) shows the relaxation dynamics of such electron and hole pockets delimited with the squares T1 and T2 in Fig. 3(f). Both populations decay with comparable relaxation times. Moreover, in figure S2[26] is shown that the balance between hole and electron decays is valid for regions symmetric in energy with respect to the Fermi level, even if they belong to different bands. This is true in particular at large pump-probe delays ($> 2ps$), while right after the optical excitation the high energy electrons act as a reservoir for the lower energy states: this affects the dynamics of the states closer to the Fermi level with scattering process interfering with the thermalization of the electron gas, deviating from a pure exponential decay. This behaviour resembles the decay of a simple metal, and in figure S3[26] we can confirm that the momentum-integrated electronic distribution thermalizes in a (hot) Fermi-Dirac distribution after 2 ps. Effectively, each of the various individual pockets of WTe$_2$ behaves like a "small metal", without any evidence of singular points in the proximity of the Fermi level. In

this regard, WTe$_2$ deviates from the behavior of prototype out-of-equilibrium Dirac semimetals like graphene, where bottleneck effects slow down the relaxation. Furthermore, if one looks at the behavior of the various pockets with respect to each other, one can see that after 2 ps the system presents a remarkably balanced behavior between excess electrons and holes: this confirms that persisting charge compensation between electron and hole pockets – widely regarded as the the main mechanism causing the extremely high magnetoresistance in WTe$_2$ – is still present even in an out-of-equilibrium conditions.

IV. CONCLUSIONS

To summarize, in this paper we showed the unoccupied band structure of WTe$_2$, observing the dispersion of the electron and hole pockets above the Fermi level. Analyzing the dynamics of excess electrons and holes in the proximity of the Fermi level, we determined a thermalization time of about 2ps. After this thermalization time, the various electron and hole pockets present a remarkable balance among their evolutions. This confirms that charge compensation among pockets is a distinctive feature of WTe$_2$, even out-of-equilibrium. Due also to our experimental resolution, our results could not provide any signature of the presence of a Weyl point, neither from the band structure nor from the relaxation dynamics in the time domain. More studies are required to give a clear conclusion on the topology of the band structure of WTe$_2$.

* marco.caputo@u-psud.fr

[1] B. Q. Lv, N. Xu, H. M. Weng, J. Z. Ma, P. Richard, X. C. Huang, L. X. Zhao, G. F. Chen, C. E. Matt, F. Bisti, V. N. Strocov, J. Mesot, Z. Fang, X. Dai, T. Qian, M. Shi, and H. Ding, Nature Physics **11**, 724 (2015).

[2] B. Q. Lv, H. M. Weng, B. B. Fu, X. P. Wang, H. Miao, J. Ma, P. Richard, X. C. Huang, L. X. Zhao, G. F. Chen, Z. Fang, X. Dai, T. Qian, and H. Ding, Phys. Rev. X **5**, 031013 (2015).

[3] S.-Y. Xu, I. Belopolski, N. Alidoust, M. Neupane, G. Bian, C. Zhang, R. Sankar, G. Chang, Z. Yuan, C.-C. Lee, S.-M. Huang, H. Zheng, J. Ma, D. S. Sanchez, B. Wang, A. Bansil, F. Chou, P. P. Shibayev, H. Lin, S. Jia, and M. Z. Hasan, Science **349**, 613 (2015).

[4] Z. K. Liu, L. X. Yang, Y. Sun, T. Zhang, H. Peng, H. F. Yang, C. Chen, Y. Zhang, Y. F. Guo, D. Prabhakaran, M. Schmidt, Z. Hussain, S.-K. Mo, C. Felser, B. Yan, and Y. L. Chen, Nature Materials **15**, 27 (2015).

[5] X. Wan, A. M. Turner, A. Vishwanath, and S. Y. Savrasov, Phys. Rev. B **83**, 205101 (2011).

[6] A. A. Soluyanov, D. Gresch, Z. Wang, Q. Wu, M. Troyer, X. Dai, and B. A. Bernevig, Nature **527**, 495 (2015).

[7] Y. Sun, S.-C. Wu, M. N. Ali, C. Felser, and B. Yan, Phys. Rev. B **92**, 161107 (2015).

[8] G. Autès, D. Gresch, M. Troyer, A. A. Soluyanov, and O. V. Yazyev, Phys. Rev. Lett. **117**, 066402 (2016).

[9] I. Pletikosić, M. N. Ali, A. V. Fedorov, R. J. Cava, and T. Valla, Phys. Rev. Lett. **113**, 216601 (2014).

[10] C. Wang, Y. Zhang, J. Huang, S. Nie, G. Liu, A. Liang, Y. Zhang, B. Shen, J. Liu, C. Hu, Y. Ding, D. Liu, Y. Hu, S. He, L. Zhao, L. Yu, J. Hu, J. Wei, Z. Mao, Y. Shi, X. Jia, F. Zhang, S. Zhang, F. Yang, Z. Wang, Q. Peng, H. Weng, X. Dai, Z. Fang, Z. Xu, C. Chen, and X. J. Zhou, Phys. Rev. B **94**, 241119 (2016).

[11] F. Y. Bruno, A. Tamai, Q. S. Wu, I. Cucchi, C. Barreteau, A. de la Torre, S. McKeown Walker, S. Riccò, Z. Wang, T. K. Kim, M. Hoesch, M. Shi, N. C. Plumb, E. Giannini, A. A. Soluyanov, and F. Baumberger, Phys. Rev. B **94**, 121112 (2016).

[12] Y. Wu, D. Mou, N. H. Jo, K. Sun, L. Huang, S. L. Bud'ko, P. C. Canfield, and A. Kaminski, Phys. Rev. B **94**, 121113 (2016).

[13] Y. Wu, L.-L. Wang, E. Mun, D. D. Johnson, D. Mou, L. Huang, Y. Lee, S. L. Bud'ko, P. C. Canfield, and A. Kaminski, Nature Physics **12**, 667 (2016).

[14] D. Di Sante, P. K. Das, C. Bigi, Z. Ergönenc, N. Gürtler, J. A. Krieger, T. Schmitt, M. N. Ali, G. Rossi, R. Thomale, C. Franchini, S. Picozzi, J. Fujii, V. N. Strocov, G. Sangiovanni, I. Vobornik, R. J. Cava, and G. Panaccione, Phys. Rev. Lett. **119**, 026403 (2017).

[15] T.-R. Chang, S.-Y. Xu, G. Chang, C.-C. Lee, S.-M. Huang, B. Wang, G. Bian, H. Zheng, D. S. Sanchez, I. Belopolski, N. Alidoust, M. Neupane, A. Bansil, H.-T. Jeng, H. Lin, and M. Zahid Hasan, Nature Communications **7**, 10639 (2016).

[16] K. Deng, G. Wan, P. Deng, K. Zhang, S. Ding, E. Wang, M. Yan, H. Huang, H. Zhang, Z. Xu, J. Denlinger, A. Fedorov, H. Yang, W. Duan, H. Yao, Y. Wu, S. Fan, H. Zhang, X. Chen, and S. Zhou, Nature Physics **12**, 1105 (2016).

[17] L. Huang, T. M. McCormick, M. Ochi, Z. Zhao, M.-T. Suzuki, R. Arita, Y. Wu, D. Mou, H. Cao, J. Yan, N. Trivedi, and A. Kaminski, Nature Materials **15**, 1155 (2016).

[18] A. Tamai, Q. S. Wu, I. Cucchi, F. Y. Bruno, S. Riccò, T. K. Kim, M. Hoesch, C. Barreteau, E. Giannini, C. Besnard, A. A. Soluyanov, and F. Baumberger, Phys. Rev. X **6**, 031021 (2016).

[19] B. Feng, Y.-H. Chan, Y. Feng, R.-Y. Liu, M.-Y. Chou, K. Kuroda, K. Yaji, A. Harasawa, P. Moras, A. Barinov, W. Malaeb, C. Bareille, T. Kondo, S. Shin, F. Komori, T.-C. Chiang, Y. Shi, and I. Matsuda, Phys. Rev. B **94**, 195134 (2016).

[20] I. Belopolski, S.-Y. Xu, Y. Ishida, X. Pan, P. Yu, D. S. Sanchez, H. Zheng, M. Neupane, N. Alidoust, G. Chang, T.-R. Chang, Y. Wu, G. Bian, S.-M. Huang, C.-C. Lee, D. Mou, L. Huang, Y. Song, B. Wang, G. Wang, Y.-W. Yeh, N. Yao, J. E. Rault, P. Le Fèvre, F. Bertran, H.-T. Jeng, T. Kondo, A. Kaminski, H. Lin, Z. Liu, F. Song, S. Shin, and M. Z. Hasan, Phys. Rev. B **94**, 085127 (2016).

[21] A. Liang, J. Huang, S. Nie, Y. Ding, Q. Gao, C. Hu, S. He, Y. Y. Zhang, C. Wang, B. Shen, J. Liu, P. Ai, L. Yu, X. Sun, W. Zhao, S. Lv, D. Liu, C. Li, Y. Y. Zhang, Y. Hu, Y. Xu, L. Zhao, G. Liu, Z. Mao, X. Jia, F. Zhang, S. Zhang, F. Yang, Z. Wang, Q. Peng, H. Weng, X. Dai, Z. Fang, Z. Xu, C. Chen, and X. J. Zhou, arXiv , 1 (2016), arXiv:1604.01706.

[22] T. Liang, Q. Gibson, M. N. Ali, M. Liu, R. J. Cava, and N. P. Ong, Nature Materials **14**, 280 (2014).

[23] C. Shekhar, A. K. Nayak, Y. Sun, M. Schmidt, M. Nicklas, I. Leermakers, U. Zeitler, Y. Skourski, J. Wosnitza, Z. Liu, Y. Chen, W. Schnelle, H. Borrmann, Y. Grin, C. Felser, and B. Yan, Nature Physics **11**, 645 (2015).

[24] M. N. Ali, J. Xiong, S. Flynn, J. Tao, Q. D. Gibson, L. M. Schoop, T. Liang, N. Haldolaarachchige, M. Hirschberger, N. P. Ong, and R. J. Cava, Nature **514**, 205 (2014).

[25] J. Faure, J. Mauchain, E. Papalazarou, W. Yan, J. Pinon, M. Marsi, and L. Perfetti, Review of Scientific Instruments **83**, 043109 (2012).

[26] See Supplemental Material at [URL] for a video showing the dispersion of the electron pockets above the Fermi level, the region used to integrate the band population shown in figure 3, an anlaysis of the time-dependent population in band V, and an analysis of the angle-integrated electron distribution.

[27] P. K. Das, D. Di Sante, I. Vobornik, J. Fujii, T. Okuda, E. Bruyer, A. Gyenis, B. E. Feldman, J. Tao, R. Ciancio, G. Rossi, M. N. Ali, S. Picozzi, A. Yadzani, G. Panaccione, and R. J. Cava, Nature Communications **7**, 10847 (2016).

[28] M. Hajlaoui, E. Papalazarou, J. Mauchain, L. Perfetti, A. Taleb-Ibrahimi, F. Navarin, M. Monteverde, P. Auban-Senzier, C. R. Pasquier, N. Moisan, D. Boschetto, M. Neupane, M. Z. Hasan, T. Durakiewicz, Z. Jiang, Y. Xu, I. Miotkowski, Y. P. Chen, S. Jia, H. W. Ji, R. J. Cava, and M. Marsi, Nature Communications **5**, 3003 (2014).

[29] M. Hajlaoui, E. Papalazarou, J. Mauchain, G. Lantz, N. Moisan, D. Boschetto, Z. Jiang, I. Miotkowski, Y. P. Chen, A. Taleb-Ibrahimi, L. Perfetti, and M. Marsi, Nano Letters **12**, 3532 (2012).

[30] J. A. Sobota, S. Yang, J. G. Analytis, Y. L. Chen, I. R. Fisher, P. S. Kirchmann, and Z.-X. Shen, Phys. Rev. Lett. **108**, 117403 (2012).

[31] Y. M. Dai, J. Bowlan, H. Li, H. Miao, S. F. Wu, W. D. Kong, P. Richard, Y. G. Shi, S. A. Trugman, J.-X. Zhu, H. Ding, A. J. Taylor, D. A. Yarotski, and R. P. Prasankumar, Phys. Rev. B **92**, 161104 (2015).

[32] W. S. Fann, R. Storz, H. W. K. Tom, and J. Bokor, Phys. Rev. B **46**, 13592 (1992).

[33] I. Gierz, J. C. Petersen, M. Mitrano, C. Cacho, I. C. E. Turcu, E. Springate, A. Stöhr, A. Köhler, U. Starke, and A. Cavalleri, Nature Materials **12**, 1119 (2013).

[34] J. C. Johannsen, S. Ulstrup, F. Cilento, A. Crepaldi, M. Zacchigna, C. Cacho, I. C. E. Turcu, E. Springate, F. Fromm, C. Raidel, T. Seyller, F. Parmigiani, M. Grioni, and P. Hofmann, Phys. Rev. Lett. **111**, 027403 (2013).